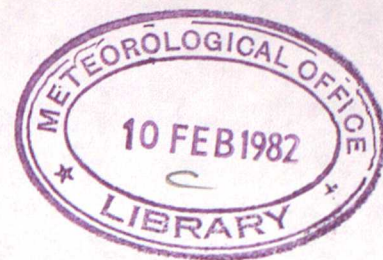


METEOROLOGICAL OFFICE

London Road, Bracknell, Berks.



136733

MET.O.15 INTERNAL REPORT

No 16

DESCRIPTION AND OPTIMISATION OF THE LOCATE TRACKING
ALGORITHM FOR USE WITH LORAN C

by

P Ryder

April 1976

Cloud Physics Branch (Met.O.15)

1. Introduction

This report investigates the characteristics of the tracking algorithms used by Beukers Labs Inc in their LOCATE windfinding equipment. The need for this investigation arises from the projected use of LOCATE equipment in the MRF C.130 to track the Met.0.15 dropsonde through re-transmitted Loran C. The analysis is carried out specifically for Loran C but the general conclusions have a wider application.

Loran C transmissions consist of groups of 8 pulses of 100 KHz carrier (9 in the case of the master transmission in a given chain). The pulses within a group are 1 millisecond apart and the group repetition rate is approximately 10 Hz but the actual rate is specific to each Loran C chain. The positional information required to track an object is derived from the difference in time of arrival at the object of some identifiable feature of the transmissions from at least 3 Loran C sources taken in pairs. The identifiable feature used in LOCATE equipment is the zero crossing of a negative going edge of a square wave derived from the Loran C carrier by amplification to limiting after band pass filtering around 100 KHz.

The basic problem is to maintain identification of the chosen zero crossings and to measure their times of arrival (TOAs) against a stable time base. Beukers use a dedicated digital computer under software control to sample signal polarity at the chosen zero crossing and use the measured average polarity to correct the sample time. This time is then the best estimate of the TOA. One zero crossing is sampled in each of the 8 pulses providing 8 polarity measurements per group. If a negative polarity is assigned a value -1 and a positive polarity is assigned +1 then the sum for the group (designated SRA) may be any even number in the range -8 to +8 with an expected value of 0 if the sample time coincides with the TOA of the zero crossing. The basic tracking equations are

$$VEL_i = VEL_{i-1} + K_v \cdot SRA_i \quad \text{--- (1)}$$

$$TOA_i = TOA_{i-1} + K_p \cdot SRA_i + VEL_i \quad \text{--- (2)}$$

where the subscript i denotes the element in the group time series.

By using the zero crossing on a negative going edge a consistently late estimate of TOA will produce a net negative for SRA to drive the TOA to earlier times. The coefficient K_p governs the response of TOA to this error signal.

The term VEL can best be understood as an integral of SRA up to the current sample time and is designed to correct for a consistently increasing TOA as experienced by the receiver moving at constant velocity for example. The coefficient K_v governs the response of VEL to SRA.

The remainder of this report describes the quantitative role of K_p and K_v in the presence of noise on the received signal both analytically and by simulation.

2.1 The phase jitter exemplified by a constant frequency signal with superimposed narrow band noise.

The hard limited signal upon which polarity samples are made contains the signal and superimposed noise within the relatively narrow frequency band of the receiver. If it is assumed that this noise is a random variable whose phase and amplitude are relatively slowly varying functions of time compared with the signal frequency (from the action of the narrow band pass filter) then the basic theory of the narrow band Gaussian Random process as described by Davenport and Root (1958) for example may be followed. This approach has been used by Poppe (1974) in his analysis of Omega Signal algorithms as applied to LO-CATE equipment.

The probability that a zero crossing will occur at Θ radians displaced from its zero noise position is given by

$$P(\Theta) = \frac{1}{2\pi} \left[e^{-SNR} + \sqrt{2SNR} \cos \Theta e^{-SNR \sin^2 \Theta} \int_{-\infty}^{\sqrt{2SNR} \cos \Theta} e^{-x^2/2} dx \right]$$

where SNR is the ratio of the signal to noise power.

Thus $SNR = \frac{A^2}{2N^2}$ where A is the amplitude of the signal and N^2 is the variance of the noise amplitude.

The integral $\int_{-\infty}^{\sqrt{2SNR} \cos \Theta} e^{-x^2/2} dx = \sqrt{\frac{\pi}{2}} (1 + \text{erf}(\sqrt{SNR} \cos \Theta))$

Thus $P(\Theta) = \frac{1}{2\pi} \left[e^{-SNR} + \sqrt{\pi \cdot SNR} \cdot \cos \Theta \cdot e^{-SNR \sin^2 \Theta} (1 + \text{erf}(\sqrt{SNR} \cos \Theta)) \right]$

This is evaluated for SNR in the range + 10 to - 14 dB in figure 1.

The probability of an error of ϕ or less is given by:

$$P'(\leq \phi) = 2 \int_0^{\phi} P(\theta) d\theta \text{ and is shown in figure 2.}$$

The RMS phase error appropriate to a given SNR may be evaluated from

$$\phi_{RMS} = \left[2 \int_0^{\pi} \theta^2 \cdot P(\theta) d\theta \right]^{1/2} \text{ and this is listed in table 1.}$$

By evaluating the integral normalised distribution $\frac{2}{\phi_{RMS}} \int_0^{\phi} P(\theta) d\theta$ and comparing this with the normalised Gaussian distribution - see figure 3, we see that, for large SNR at least, the probability of a given error may be approximated to by a Gaussian distribution with mean zero and standard deviation as listed in table 1 for the appropriate SNR. This approximation is used in the simulation described in section 3. The expected average value of SRA as a function of error ϕ may also be calculated as follows:

If the expected TOA is displaced ϕ from the true zero crossing then the probability of the sample experiencing a polarity + 1 is :

$$P_+(\phi) = \int_{\phi}^{\pi-\phi} P(\theta) d\theta = \int_0^{\phi} P(\theta) d\theta + \int_0^{\pi-\phi} P(\theta) d\theta$$

and the probability of - 1 is

$$P_-(\phi) = 1 - P_+(\phi)$$

Thus the expected value of SRA for the given ϕ and SNR is :

$$\begin{aligned} P''(SRA)_{\phi, SNR} &= 8 \times [P_+(\phi) - P_-(\phi)] \\ &= 8 \times \left[2 \int_0^{\phi} P(\theta) d\theta + 2 \int_0^{\pi-\phi} P(\theta) d\theta - 1 \right] \end{aligned}$$

This has been evaluated for a range of SNRs and the results are shown in figure 4, for the positive half cycle.

The gradient $\frac{d(SRA)}{d\phi}$ is a measure of the sensitivity of the polarity error to phase error ϕ . This quantity is clearly a function of ϕ and SNR. Thus at large signal to noise ratios a small error $\pm \phi$ will give an average SRA close to the maximum ± 8 but at low SNRs quite large errors in phase will give average SRAs considerably less than ± 8 . Nevertheless if we assume that the phase jitter is largely due to noise (and we shall see in section 3 that this is a reasonable approximation) then the probability of achieving an error ϕ in the knee region of any of the curves shown in figure 4 is quite small and we may calculate an average sensitivity $\left[\frac{d(SRA)}{d\phi} \right]_{SNR}$ from

$$\left[\frac{d(SRA)}{d\phi} \right]_{SNR} = \int_0^{\pi} P(\phi)_{SNR} \cdot \frac{P''(SRA)_{\phi, SNR}}{\phi} d\phi$$

The results are listed in table 2, and it is clear that the average sensitivity is close to the initial slope of the curves in figure 4. This approximation is useful as it allows pseudo-linearisation of the tracking equations. Its validity is tested by comparing theory and simulation in section 3.

2.2 Response of the tracking equations.

Equations (1) and (2) can be combined to give :

$$TOA_i - TOA_{i-1} = K_p \cdot SRA_i + K_v \cdot \sum_{j=1}^i SRA_j$$

If the TOA in the absence of noise is varying with time as $TOA = f(t)$ and the measured TOA is TOA_i then

$$TOA_i = f(t) + \phi(t)$$

and $TOA_{i-1} = f(t - \Delta t) + \phi(t - \Delta t)$ where Δt is the time between groups of the 8 Loran C pulses (typically $\Delta t = 0.1$ sec)

then $TOA_i - TOA_{i-1} = f(t) - f(t - \Delta t) + \phi(t) - \phi(t - \Delta t)$ and recalling that the negative going slope zero crossing is used so that $\left[\frac{d(SRA)}{d\phi} \right]_{SNR}$ is less than zero.

$$f(t) - f(t - \Delta t) + \phi(t) - \phi(t - \Delta t) = -K_p \left| \frac{d(SRA)}{d\phi} \right|_{SNR} \phi(t) - K_v \left| \frac{d(SRA)}{d\phi} \right|_{SNR} \int_0^t \phi(t) dt$$

then dividing through by Δt and using the approximations

$$\frac{1}{\Delta t} (f(t) - f(t - \Delta t) + \phi(t) - \phi(t - \Delta t)) = \frac{d(f + \phi)}{dt}$$

$$\text{and } \int_0^t \phi(t) \Delta t = \int_0^t \phi(t) dt$$

$$\text{we have } \frac{d(f + \phi)}{dt} = -\frac{K_p}{\Delta t} \left| \frac{d(SRA)}{d\phi} \right|_{SNR} \phi - \frac{K_v}{\Delta t^2} \left| \frac{d(SRA)}{d\phi} \right|_{SNR} \int_0^t \phi dt$$

and differentiating

$$\frac{d^2(f + \phi)}{dt^2} = -\frac{K_p}{\Delta t} \left| \frac{d(SRA)}{d\phi} \right|_{SNR} \frac{d\phi}{dt} - \frac{K_v}{\Delta t^2} \left| \frac{d(SRA)}{d\phi} \right|_{SNR} \phi \quad \text{--- (3)}$$

$$\text{If } \alpha = \frac{K_p}{\Delta t} \left| \frac{d(SRA)}{d\phi} \right|_{SNR} \quad \text{and} \quad \beta = \frac{K_v}{\Delta t^2} \left| \frac{d(SRA)}{d\phi} \right|_{SNR}$$

$$\text{then } \frac{d^2(\phi)}{dt^2} + \alpha \frac{d\phi}{dt} + \beta \phi = -\frac{d^2(f)}{dt^2} \quad \text{--- (4)}$$

Assuming $f = 0$ for the moment so that the system response under steady but noisy conditions may be investigated

$$\frac{d^2\phi}{dt^2} + \alpha \frac{d\phi}{dt} + \beta \phi = 0 \quad \text{--- (5)}$$

This has solutions of the form

$$\begin{aligned} \text{when } \beta > \frac{\alpha^2}{4} \quad \phi &= e^{-\frac{\alpha t}{2}} (A \cos(\sqrt{\beta - \frac{\alpha^2}{4}} t) + B \sin(\sqrt{\beta - \frac{\alpha^2}{4}} t)) \\ \beta = \frac{\alpha^2}{4} \quad \phi &= e^{-\frac{\alpha t}{2}} (A + Bt) \\ \beta < \frac{\alpha^2}{4} \quad \phi &= A e^{-(\frac{\alpha}{2} - \sqrt{\frac{\alpha^2}{4} - \beta})t} + B e^{-(\frac{\alpha}{2} + \sqrt{\frac{\alpha^2}{4} - \beta})t} \end{aligned}$$

i.e. the solutions are underdamped, critically damped and overdamped respectively.

Thus to optimise the speed of response and to prevent instability as exemplified by an oscillatory response we should set

$$4\beta = \alpha^2 \quad \text{or} \quad 4k_v = k_p^2 \left| \frac{d(\text{SRA})}{d\phi} \right|_{\text{SNR}}$$

Obviously this condition can only be met for one particular SNR as $\left| \frac{d(\text{SRA})}{d\phi} \right|_{\text{SNR}}$ is a function of SNR. The response will be overdamped or underdamped depending upon whether the actual SNR is greater or less than that used to set up equation 8.

We can also identify $\frac{2}{\alpha} = \frac{2 \cdot \Delta t}{k_p \left| \frac{d(\text{SRA})}{d\phi} \right|_{\text{SNR}}} = \bar{T}$, as the time constant of the critically damped solution. \bar{T} clearly decreases with increasing SNR.

It is instructive to estimate the response in the vicinity of the critical condition $4\beta = \alpha^2$. In the oscillatory case periodicities much longer than the damping time constant will be greatly attenuated.

$$\text{Let } T_p = \frac{2\pi}{\sqrt{\beta - \frac{\alpha^2}{4}}} \quad \text{— the oscillation period.}$$

$$\text{and } \bar{T} = 2/\alpha$$

then if adequate damping is achieved for $T_p \geq n\bar{T}$ where $\infty > n > 0$ we find the condition

$$\frac{\alpha^2}{4} \left(\frac{4\pi^2 + n^2}{n^2} \right) \geq \beta$$

$$\begin{aligned} \text{Thus if } n \approx 3 \quad & 5/4 \alpha^2 \geq \beta \\ n \approx 4 \quad & \alpha^2 \geq \beta \\ n \approx 5 \quad & 2/3 \alpha^2 \geq \beta \end{aligned}$$

In the overdamped case a similar analysis can be performed if we identify $\bar{T}_{\text{MAX}} = 2/(\alpha - \sqrt{\alpha^2 - 4\beta})$ and again $\bar{T} = 2/\alpha$. Thus with the condition $\bar{T}_{\text{MAX}} \leq m\bar{T}$ where $m > 1$ we find

$$\beta \geq \frac{\alpha^2}{4} \left(\frac{2m-1}{m^2} \right)$$

Thus if $m = 1.5$ $\beta \geq 0.9 \frac{\alpha^2}{4}$
 $m = 2$ $\beta \geq 0.75 \frac{\alpha^2}{4}$

Therefore we may express the composite condition

$$\frac{\alpha^2}{4} \left(\frac{4\pi^2 + n^2}{n^2} \right) \geq \beta \geq \frac{\alpha^2}{4} \left(\frac{2m-1}{m^2} \right) \quad \text{where in the limit } n \rightarrow \infty, m \rightarrow 1$$

Possible choices of n and m are investigated in section 3.

Rewriting equation 4 assuming $\alpha^2 = 4\beta$ and using the parameter $\bar{T} = 2/\alpha$ we have

$$\frac{d^2\phi}{dt^2} + \frac{2d\phi}{\bar{T}dt} + \frac{1}{\bar{T}^2}\phi = -\frac{d^2f}{dt^2}$$

Now if $f(t) = \frac{1}{2} a t^2$ i.e. the tracked object experiences a constant acceleration of a , then with the boundary condition $\phi = 0$ when $t = 0$ we find

$$\phi = \frac{1}{2} a \bar{T}^2 (e^{-t/\bar{T}} - 1) \quad \text{--- (6)}$$

Thus if $a = 10 \text{ m/sec}^2 = 1 \text{ g}$ and $\bar{T} = 5$ seconds we find that the estimated TOA will lag by the equivalent of 125 m after the transient response has died away. If \bar{T} is 2 seconds this steady state lag falls to 20 metres.

During accelerations the system response may be inadequate to maintain acquisition of the chosen zero crossing. For example, if the sample time continually lags behind the true TOA then a point may be reached when, because the polarity signals are periodic (see equation 7), the system is driven backwards to the previous negative going zero crossing. This is known as 'loss of lock' or in navigational terms 'lane skipping'.

The analysis based on equation (4) is valid only if noise provides the major contribution to the error signal. Specifically the use of the error ϕ in this equation is possible only because of our pseudo-linearisation through the use of $\left| \frac{d(SRA)}{d\phi} \right|_{swe}$. This is becoming increasingly invalid as $\phi \rightarrow 2.5 \mu \text{ secs}$ (see figure 4) and for $\phi > 2.5 \mu \text{ secs}$ $\frac{d(SRA)}{d\phi}$ changes sign to drive the sample time in the wrong direction. However, we may estimate the limiting condition. In the vicinity of $\phi = 2.5 \mu \text{ sec}$ SRA will assume a maximum value so that the velocity and acceleration terms equivalent to $\frac{d^2\phi}{dt^2}$ and $\frac{d\phi}{dt}$ will tend to zero. Therefore the remaining term must be capable alone of matching the imposed acceleration. Thus $\frac{K_v}{\Delta t^2} \text{SRA}_{\text{max}} \geq \frac{d^2f'}{dt^2}$ where $\frac{d^2f'}{dt^2}$ is the acceleration of the true TOA. Hence if the maximum likely acceleration is 10 m/sec^2 then $\frac{d^2f'}{dt^2} = 0.033 \mu \text{ secs/sec}^2$. For SNR = 0 dB the expected average maximum value of SRA is ~ 6.7 (see figure 4) and hence $K_v_{\text{SNR} = 0} > 4.9 \cdot 10^{-5}$. A list of minimum

values of K_v for various maximum accelerations is given in table 3 as a function of SNR. These are tested in section 3.

3. Tracking simulation.

A computer program has been written to simulate the tracking equations.

The object to be tracked is constrained to be on a line between two transmitters so that only two TOAs are computed and the geometry is optimised to that of a Loran C baseline. A time step of 0.1 second is used to coincide with the nominal Loran C repetition rate. The simulated signals from the two transmitters are treated entirely separately. At each time step for each signal, the true TOA (ATOAC) is calculated from the imposed body velocity, acceleration and previous position. Each measured TOA (AMTOA) is calculated by adding an error (DT) to ATOAC. The error is generated by sampling a Gaussian distribution with mean zero and standard deviation as given in table 1 for the assumed signal to noise ratio. The Gaussian distribution is generated from the standard IBM FORTRAN sub-routine 'GAUSS' driven by the pseudo-random number generator 'RANDU'. The errors for the two signals are of course drawn separately from their respective populations. A parameter $DTOA = AMTOA - ATOA_{i-1}$ is then calculated where $ATOA_{i-1}$ is the last estimate of the appropriate TOA (i.e. the simulated zero crossing sampling time). A signal polarity measurement is generated from

$$RA = \frac{DTOA}{|DTOA|} \times (-1)^N \quad \text{where } N = \frac{|DTOA|}{5.0} \quad (7)$$

(the units of TOA etc are μ seconds)

This procedure of deriving DTOA and RA, is repeated eight times, keeping ATOAC and $ATOA_{i-1}$ constant, but using a new sample of DT each time from the respective error populations of the two signals. The sum of the eight polarity samples gives ASRA which is used to generate the new estimated value of ATOA from :

$$AVEL_i = AVEL_{i-1} + K_v \times ASRA$$

$$ATOA_i = ATOA_{i-1} + K_p \times ASRA + AVEL_i$$

The two signals produce $ATOA_i$ and $BTOA_i$ by the above procedure.

These are averaged over one second (\overline{ATOA}_j and \overline{BTOA}_j)

and the time difference is formed from $TD_j = \overline{ATOA} - \overline{BTOA}$

this is used to form an estimated body position using the scale factor of 150 m/ μ sec appropriate to the assumed base line operation. This is compared with the true body position as are estimated and true body velocities.

This program has been used to test the validity of the theory developed in section 2. In the ensuing discussion the tracked body is at rest until $t = 200$ seconds and then accelerates at 10 m/sec² to a velocity of 300m/sec² and remains at that velocity until $t = 600$ seconds at which time the simulation ceases. It is appreciated that this velocity is somewhat unrealistic but it does allow a significant period at constant acceleration to test the theory.

A typical result of a tracking simulation is shown in figure 5 for $SNR = 0$ $\tau = 5$ sec $n = \infty$ (critical damping). True and estimated positions are the average of the 10 values available each second and the error is obtained by subtracting this 1 second mean true position from the 1 second mean estimate. The acceleration lag is very apparent, as is a 30 metre offset during the constant high velocity phase. This latter arises because the effective servo mechanism of equations 1 and 2 attempts to stabilise the TOA estimate to be correct for the next sample time 0.1 second hence. Thus the estimate of position is $V \times \Delta t$ in error under steady conditions, in addition to the superimposed noise effect. This is a small error at low velocities but is quite well defined at 300 m/sec. If necessary in a particular application, this can be allowed for by correcting the time of the position estimates by Δt .

The first test of theory consists of a comparison of the TOA lag during the constant acceleration, as exemplified by simulation, with that predicted by equation 6. The results are shown in figure 6. The error bars denote the spread in lag during a simulation. Equation 6 underestimates the error as K_v decreases towards the limits defined in table 3 but there is a broad agreement between numerical experiment and theory, over the range $+10 \geq SNR \geq -10$ dB.

We next verify the lower limits on K_v given in table 3. In this test K_p was set to a value appropriate to $\tau = 10$ seconds and K_v was decreased until lock was lost. An acceleration of 10 m/sec^2 was used in all simulations. The results suggest that the figures in table 3 are, as expected from the simple analysis of section 2, rather conservative estimates of the lower limit. Lock was lost at approximately 80% of the limits suggested in table 3 for $SNR = 0$ or 10 dB and at 50% of the limit for $SNR = -10$ dB. Nevertheless, the analysis certainly provides adequate design criteria. The phenomena of 'lane skipping' or 'loss of lock' is exemplified in figure 7 for $SNR = 0$ dB $K_p = 4.4 \cdot 10^{-3}$, $K_v = 4.0 \cdot 10^{-5}$. Note the increased error scale in this figure compared with that of figure 5.

The prediction of oscillating behaviour was verified by setting $K_p = 7.33 \cdot 10^{-4}$, $K_v = 9.7 \cdot 10^{-5}$ during a simulation run in which no acceleration was imposed. This choice of coefficients produces an underdamped response of $\tau = 60$ secs and oscillating period $T_p = 30$ secs for $SNR = 0$, according to theory. The results are shown in figure 8. An oscillation with an average period of 30.8 secs is clearly identifiable.

The system response in the vicinity of the critical condition $4\beta = \alpha^2$ was established by setting $\tau = 5$ seconds, $SNR = 0$ dB and calculating the RMS position error during the first 200 seconds and during the acceleration phase of simulation

for K_v set according to the various criteria $m = 2$, $n = \infty$, $n = 3$, $n = 2$, $n = 1$. The results are listed in table 4. As n decreases, the error during the acceleration phase decreases quite considerably, but the error during the steady phase does not show any marked increase until n falls to 2 or 1. Setting $m = 2$ (overdamping) produces an insignificant improvement in the steady state error but a significant increase in the acceleration lag. Thus if the tracked body experiences significant acceleration there is a worthwhile gain to be achieved from setting up a slightly overdamped response. For design purposes the criterion $n \gg 3$ appears reasonable.

From the above comparisons it appears that the pseudo-linearisation described in section 2 does allow a reasonable analytical description of the system performance, as verified by the numerical simulation, and that its limitations (e.g. minimum value of K_v) are quantifiable. We are now in a position to generate design criteria for the system response i.e. reasoned optimisation of K_p and K_v .

4. Optimisation of Kp and Kv.

Any optimisation scheme depends upon an adequate definition of the environment in which the system is to be optimised and upon a statement of the required system performance. Therefore before considering some specific examples it is necessary to consider in more detail than in the preceding sections how the environment and performance should be defined.

(a) The effects of acceleration.

We have identified the effects of acceleration of the tracked body on the TOAs and the analysis in section 2 is of direct application to a self tracked object such as an aircraft for example. We are also concerned with the problem of tracking a remote sonde by the retransmission of Loran C on a UHF link to a mobile receiver. In this case the time of arrival is a function of both the LF transmitter - sonde distance and the sonde - receiver distance. In a simple one dimensional model of an aircraft dropping a sonde on the baseline between two transmitters such that at some time t , the sonde is p_1 from transmitter 1 and p_2 from transmitter 2 while the aircraft is a distance d from the sonde then

$$TOA_1 = (p_1 + d)/c$$

$$TOA_2 = (p_2 + d)/c$$

where any phase shifts in the sonde, which should certainly be constant, have been neglected. At first sight it appears that the sonde aircraft distance d is unimportant as it cancels in the formation of time differences. However, the TOAs are independently tracked so that for example a sonde moving towards transmitter 1 along the base line will produce an essentially constant TOA_1 at a static receiver and TOA_2 will increase because of an increase in both p_2 and d . Even in a situation where acceleration in d far exceeds acceleration in p (due to movement of the UHF receiver) cancellation will not be exact unless both tracking algorithms exhibit the same response to acceleration. In section 2 we showed that a constant lag of $\frac{1}{2} a T^2$ was eventually achieved under constant acceleration a , for critical damping. Thus to remove dependence on d in the time difference, T should be identical for both algorithms. Figure 9 demonstrates that this cannot be achieved for a particular choice of Kp if the two SNRs are different from one another.

Thus the accelerations likely to be experienced by both the tracked and UHF receiving/analysing bodies are of importance in any optimisation scheme.

(b) The effects of signal to noise ratio.

We have established the dependence of the constants α and β upon the signal to noise ratio. This arises directly from the use of a polarity detection servo-mechanism and is not a feature of a linear servo for example. Optimisation depends upon a knowledge of the SNRs likely to be experienced as we have seen above. We should, however, note that the dependence of α and β on SNR does serve to reduce the range of RMS position errors experienced for a given choice of K_p and K_v over a range of SNRs. The fact that \bar{T} increases with decreasing SNR in figure 9 (leading to increased smoothing as the noise increases) demonstrates this feature. We must therefore be aware of the likely range of SNRs in the operating area and expect, in general, to set up the tracking algorithms through K_p and K_v for each signal separately.

(c) System performance.

In the preceding sections of this report we have used position errors as a means of defining the performance of the system. In practice it is the time derivative of position error which is most relevant to wind finding, and we should seek to optimise for minimum error in the band of the error frequency spectrum which contains the meteorologically significant data. This in turn impinges upon a range of problems not suited to this report such as optimum sonde fall speed, representivity of measurements at a point, significance of features as a function of their scale, etc. It does, however, seem clear that we should (a) not over-smooth the data so that possibly significant data are removed or large isolated errors are aliased into the output time series (b) not allow motion of the aircraft (for example) to influence the tracking data. This approach allows the problem of filtering the time series to be solved at a later stage.

We may now define a set of general design criteria as follows :

1) To avoid poor response under acceleration of the tracked body and/or to avoid the insertion of errors into the data from acceleration of the tracking body (e.g. aircraft) the effective time constant should be maintained at as low a value as is necessary to achieve a lag error ($\frac{1}{2} \alpha \bar{T}^2$ for critical damping - see equation 6) which is comparable with the RMS error under steady state conditions. The RMS position errors obtained during simulation runs for a stationary body are shown in figure 10 as a function of SNR, and time constant \bar{T} for both critical and underdamping ($n = 3$). Comparing these data with figure 6, we see that \bar{T} should be 2 to 3 seconds for a $\sim 10 \text{ m sec}^{-2}$ and $-10 \leq \text{SNR} \leq 10 \text{ dB}$.

2) To avoid significant oscillatory response we suggest the criterion

$$\frac{K_p^2}{4} \left| \frac{\partial \overline{SRA}}{\partial \phi} \right|_{SNR} \geq K_v \left(\frac{n^2}{4\pi^2 + n^2} \right) \quad \text{with } n = 3 \text{ for the minimum expected value of } \left| \frac{\partial \overline{SRA}}{\partial \phi} \right|_{SNR}, \text{ i.e. for the lowest expected SNR.}$$

Thus $K_v \leq 1.347 K_p^2 \left| \frac{\partial \overline{SRA}}{\partial \phi} \right|_{SNR}$ with the equality used for the lowest likely SNR. This criterion must however be subject to the condition that, given the maximum likely TOA acceleration, K_v should not be significantly lower than the limits given in table 3, to avoid 'lane skipping'.

Figure 11 is a useful optimisation nomogram showing the relationship between K_p and K_v for critical damping at a range of SNRs. An operating point to the right of a constant SNR locus corresponds to underdamping for that SNR and a point to the left produces over damping. Thus $K_p = 2.2 \cdot 10^{-2}$, $K_v = 5.5 \cdot 10^{-4}$ corresponds to critical damping with a time constant of 2 seconds for signals with SNR = 0 dB; to underdamping with $\overline{T} = 7.5$, $n \approx 4$ for SNR = -10 dB and to overdamping with $\overline{T} = 0.6$ sec, $m = 6$ for SNR = +10 dB.

Example 1. It is required to track an aircraft travelling at a true air speed of 150 m/sec, capable of executing up to rate 2 turns ($6^\circ/\text{sec}$) where the minimum expected SNR is -10 dB and the average for both signals is 0 dB. The quoted rate of turn implies that the one dimensional velocity of the aircraft can reduce from 150 m/sec to zero in 15 seconds (the time taken to turn through 90°).

This is an average deceleration of 10 m/sec^2 . Thus the displacement error will be $\sim 5 \overline{T}^2$ for critical damping. From figure 10 the average SNR of 0 dB will produce, under constant velocity conditions, RMS errors of 20 to 30 m. To maintain a comparable acceleration error $\overline{T} \sim 2$ seconds and $K_p \approx 2.2 \cdot 10^{-2}$. We may now determine K_v from the requirement that $n = 3$ for the minimum SNR -10 dB, giving $K_v = 8.06 \cdot 10^{-4}$. Inspection of figure 11 shows that the working point so defined gives slight underdamping for SNR = 0, and slight overdamping for SNR = +10 dB and that K_v exceeds the minimum required to maintain lock at the stated maximum acceleration. The RMS errors during the static phase of the simulation were 61, 30 and 11 metres and 91, 41 and 14 metres during and shortly after the acceleration phase for -10, 0 and +10 dB respectively. Note that the ratio of the static RMS errors for ± 10 dB is approximately 5.5. A comparable linear servo, in which \overline{T} is independent of SNR, is expected, from the data of figure 10, to produce a ratio of ~ 10 . (see discussion in 4(b) above)

Example 2 To track a balloon borne sonde rising at 6 m/sec when the re-transmitted data are received at a static site. It is known that maximum likely wind shear in the atmosphere is 0.05 sec^{-1} and that the signal to noise ratios of the two transmitters used are -4 dB and +6 dB. For simplicity we will assume that the receiving site is on the baseline at the launch point and that all motion is along the baseline. The ascent rate and maximum shear imply a maximum horizontal acceleration of 0.3 m sec^{-2} . However, there is an additional acceleration at launch as the sonde vertical velocity increases from 0 to 6 m/sec. Simple mechanics suggest (a) an initial acceleration of 0.5 g for a 4 Kgm payload + balloon with a typical free lift of 2 Kgm and (b) that 90% of the 'terminal' vertical velocity will be achieved within ~ 2 seconds. Therefore for computational purposes we will assume an average acceleration of 3 m sec^{-2} lasting for 2 seconds after launch.

Initially at least we will ignore this short duration acceleration and design for a maximum error of 0.3 m sec^{-2} . From figure 10 a time constant, $T = 10$ seconds is compatible with such an acceleration. Despite the implication that the SNRs are constant, in practice we design for a slight amount of underdamping so that small changes in signal strength maintain our design criterion of $n \geq 3$. Accordingly we set up K_p and K_v for $n = 5$ thus :

$$\begin{array}{lll} \text{SNR} = -4 \text{ dB} & K_p = 7.35 \cdot 10^{-3}, & K_v = 9.5 \cdot 10^{-5} \\ \text{SNR} = +6 \text{ dB} & K_p = 2.13 \cdot 10^{-3}, & K_v = 2.7 \cdot 10^{-5} \end{array}$$

A flight was simulated by setting a vertical acceleration of 3 m sec^{-2} for the first 2 seconds and horizontal acceleration of 0.3 m sec^{-2} from $t = 100$ to 200 seconds and -0.3 m sec^{-2} from $t = 300$ to 500 seconds. (Positive acceleration, velocity etc. are towards the transmitter of the 6 dB signal). The time series of position error is shown in figure 12. There is very little evidence of any of the accelerations mapping through into this time series.

Example 3 To track an aircraft dropsonde falling in still air from a manouvering aircraft. We will assume that the aircraft drops the sonde while travelling along the baseline at 150 m/sec, and that 100 secs later it makes a 180° turn at $3^\circ/\text{sec}$ onto a reciprocal track (neglecting the movement off the baseline). We will further assume that the sonde is 60 m beneath the aircraft falling vertically at the moment of acquisition. Initially we will use the aircraft tracking data at 6 secs after launch for the starting point of sonde tracking but will subsequently investigate

methods of improving the starting point. We will assume that Loran C transmissions are received at the aircraft after the re-transmission from the sonde with average SNRs of + 6 dB from station 1 and - 4 dB from station 2 but also investigate the effects of changing these.

The stated rate of turn is equivalent to a linear acceleration of $\sim 5 \text{ m sec}^{-2}$ so figure 10 suggests $T = 3$ seconds. If we suspect the possibility of a decreasing SNR through the sonde drop then it is sensible to set K_p and K_v for critical damping initially. Thus for

SNR = + 6 dB	$K_p = 7.1 \cdot 10^{-3}$	$K_v = 1.18 \cdot 10^{-4}$
SNR = - 4 dB	$K_p = 2.45 \cdot 10^{-2}$	$K_v = 4.08 \cdot 10^{-4}$

During the first simulation run of the above example it was found that lock was lost, during transfer from the aircraft TOAs to those from the sonde, on the signal from the transmitter ahead of the aircraft. In the six seconds between ejection of the sonde and attempting to track it the aircraft moves 900 metres. Thus a step change occurs in the TOA, of the signal from the transmitter towards which the aircraft is moving, of 6 μsec . This is due to an additional 900 m of path-length for the Loran transmission and a further 900 m (approx) for the UHF pathlength back to the aircraft. This error leads to a skip of one cycle (10 μs). The other transmission does not exhibit the effect because the UHF sonde-aircraft pathlength compensates for the reduced LF pathlength to the sonde. In general, off the baseline, the errors will lie between these two extremes of 0 and 6 μs .

As the sonde may be expected to lose its aircraft-given velocity very quickly after parachute deployment, a better starting point for sonde tracking is given by the TOAs at the moment of ejection to each of which is added a delay given by $V_{ac} \times t/c$. V_{ac} is (ideally) the aircraft ground speed, t the time between ejection and acquisition of the sonde and c is the velocity of electromagnetic radiation. Any constant phase delay produced by the sonde would in practice also be added.

This method was used in the second simulation and the resulting 1 second position errors are shown in figure 13. Lock was maintained. There is a remaining source of error at acquisition caused by the use of a zero velocity word for the sonde although both TOAs are increasing at a rate of 0.05 μsecs per 100 milliseconds due to the increasing sonde - aircraft UHF pathlength. The velocity words at acquisition were set to 0.05 in the third simulation. The resultant position error time series is shown in figure 14. Very little improvement is apparent.

This is because care was taken to match the time constants of the tracking equations so that almost equal errors were caused in d and hence cancelled in the time difference.

The fourth and fifth simulations were run with the SNRs of the two transmissions reversed with the originally allocated values of K_p and K_v . The velocity words were zero at acquisition in the fourth simulation (fig.15) and 0.05 in the fifth (fig.16). The effective time constants are no longer matched and aircraft acceleration from $t = 94$ to $t = 154$ secs maps onto the position errors. The pronounced error in the vicinity of $t = 270$ is due to the acceleration in the TOAs as the aircraft approaches, passes overhead and recedes from the sonde. In addition the fourth simulation exhibits a large error shortly after acquisition while the velocity words build up at different rates. Finally in the sixth and seventh simulations each SNR is decreased by 6 dB below the value used in the optimisation of K_p and K_v . The effective time constants tend to increase together so that aircraft motion, although just discernable in figures 17 and 18 is not as pronounced as in figures 15 and 16.

5. Conclusions

The basic theory of the Beukers Labs Inc tracking equations has been developed and the concept of pseudo-linearisation found to be both valid (within limits) and useful. A simulation program has been produced initially to test predictions of the theory but also to model complex interactions ^{inherent} in the re-transmission concept of IO-CATE. A set of optimisation criteria have been derived for the coefficients which govern the response of the tracking equations. Finally these criteria have been used in some specific examples of interest.

Refs.

Wilbur B. Davenport, Jnr. and William L. Root, "An introduction to the theory of random signals and noise". McGraw Hill (1958)

Martin C. Poppe, Jnr. "Omega signal measurement algorithms"
Final Report CE 4004 Contract No. 4 - 13701 (1974)

Appendix. Determination of SNR.

As SNR is such an important design parameter for the optimisation of K_p and K_v it is very desirable to establish its value for each Loran C signal.

As suggested by Poppe (1974), let us suppose that a second polarity sum SRA_T , (analogous to SRA) is generated from samples taken at a fixed time T after the TOA samples. Then from the data of figure 4 we may determine the average value of this sum as a function of SNR. The relationship is shown below and clearly by choosing T to be in the vicinity of 1.0 to 1.5 μ secs the average value of SRA_T may be used to infer the average SNR.

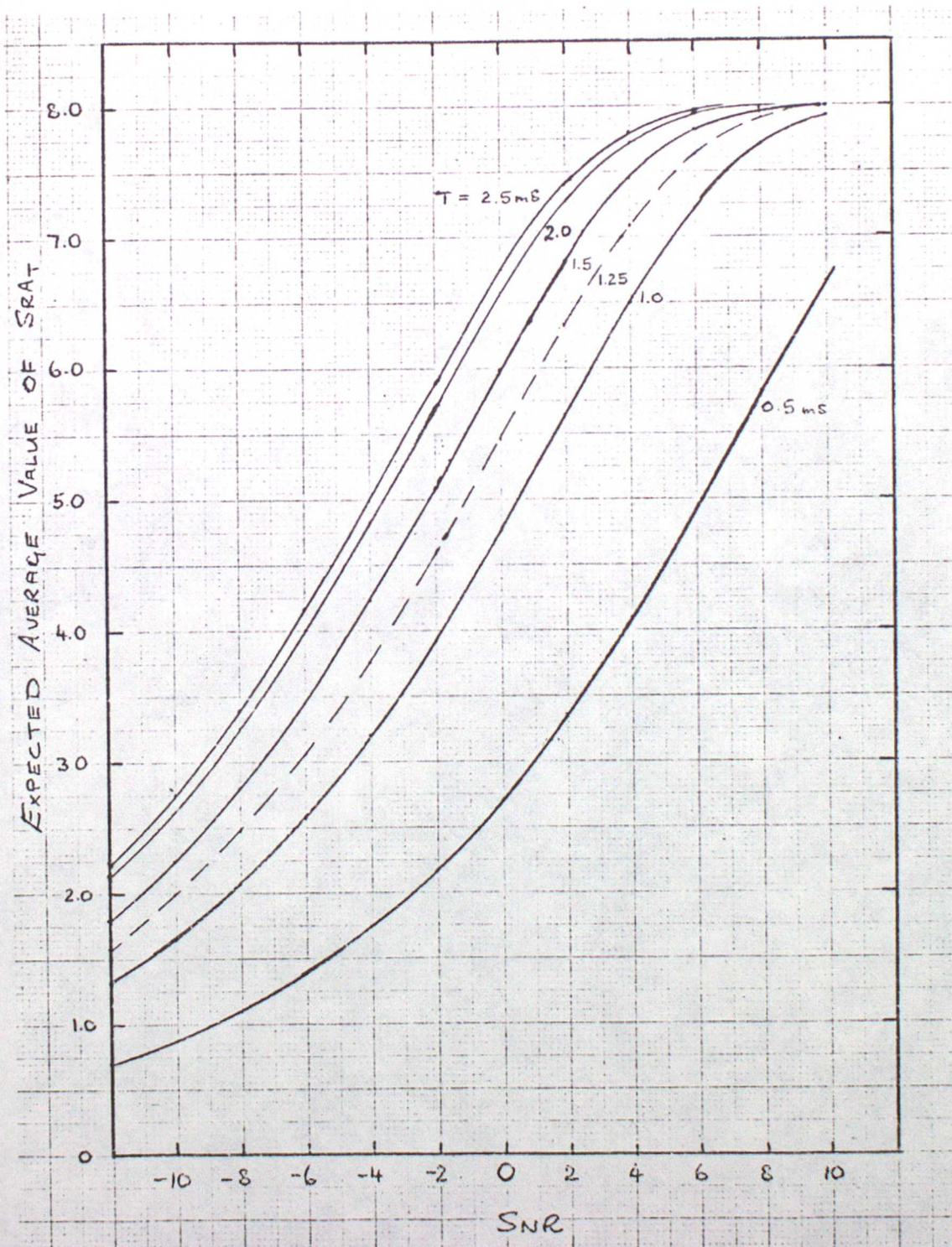


TABLE 1 Root mean square phase error as a function of signal to noise ratio.

SNR (dB)	ϕ_{RMS} (radians)	ϕ_{RMS} (μ secs)
10	0.230	0.366
8	0.297	0.473
6	0.392	0.622
4	0.527	0.839
2	0.694	1.105
0	0.871	1.39
-2	1.040	1.66
-4	1.188	1.89
-6	1.313	2.09
-8	1.415	2.25
-10	1.497	2.38
-12	1.563	2.49
-14	1.615	2.57

TABLE 2 Expected average rate of change of SRA with phase error as a function of signal to noise ratio.

SNR (dB)	$\left \frac{d(\text{SRA})}{d\phi} \right $ (μsec^{-1})
10	14.70
8	11.79
6	9.39
4	7.43
2	5.83
0	4.55
-2	3.53
-4	2.72
-6	2.09
-8	1.61
-10	1.24
-12	0.96
-14	0.74

TABLE 3 Minimum value of K_v to maintain zero crossing acquisition for various body accelerations.

SNR (dB)	SRA _{max}	Minimum K_v (in units of 10^{-5}) for stated maximum expected acceleration (m/sec^2)		
		10	5	3
10	8.0	4.1	2.1	1.3
8	8.0	4.1	2.1	1.3
6	8.0	4.1	2.1	1.3
4	7.8	4.2	2.1	1.3
2	7.4	4.5	2.2	1.4
0	6.7	4.9	2.4	1.5
-2	5.9	5.6	2.8	1.7
-4	5.0	6.6	3.3	2.0
-6	4.2	7.9	3.9	2.4
-8	3.4	9.7	4.9	2.9
-10	2.8	12	5.9	3.6
-12	2.2	15	7.5	4.5
-14	1.8	18	9.2	5.6

TABLE 4 RMS position errors in the vicinity of critical damping for SNR = 0 dB, = 5 seconds.

Criterion	Steady state RMS error (metres)	Acceleration phase RMS error (metres)
$m = 2$	19.7	226.5
$n = \infty$	20.5	190.3
$n = 3$	28.1	52.6
$n = 2$	32.8	41.0
$n = 1$	55.6	56.2

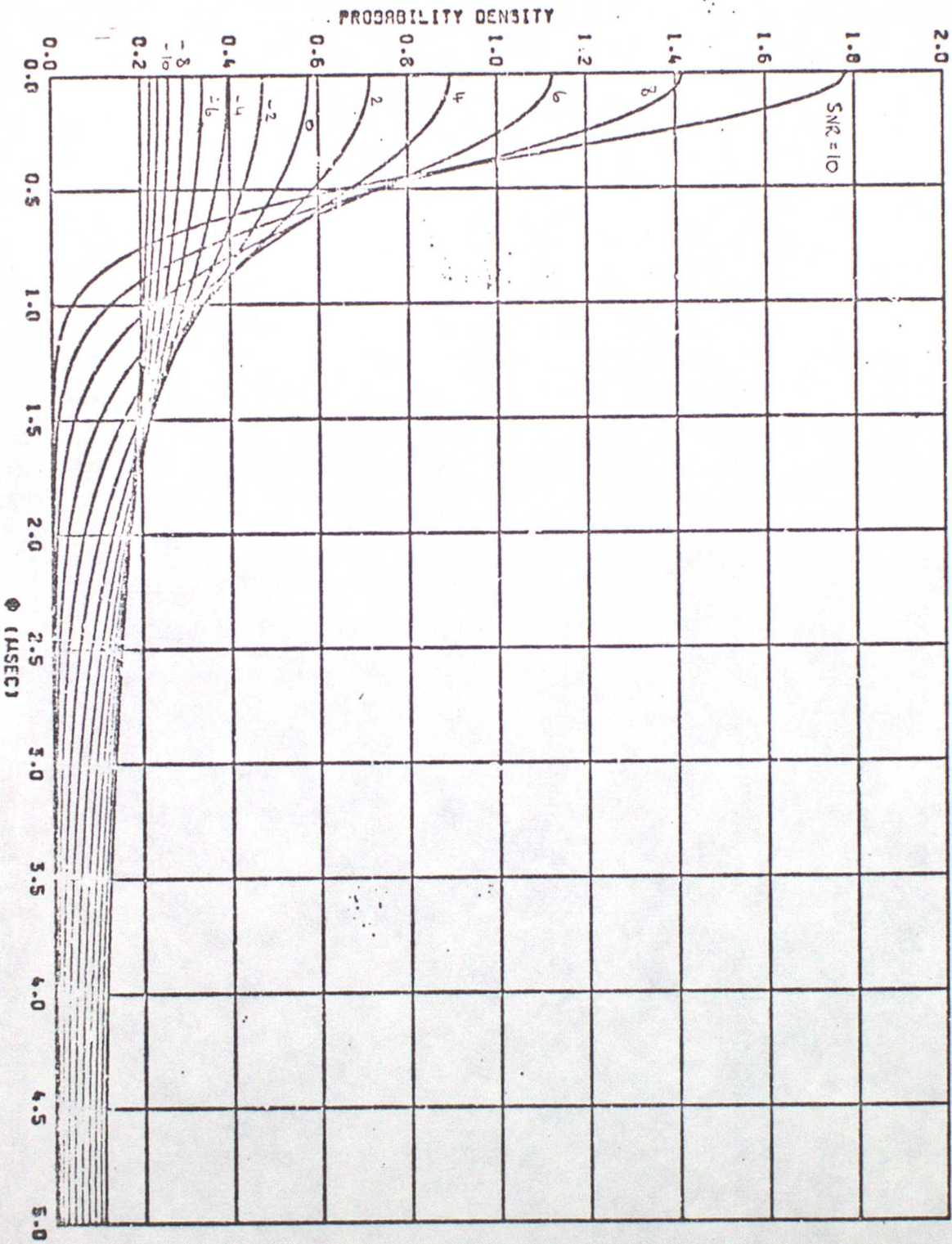
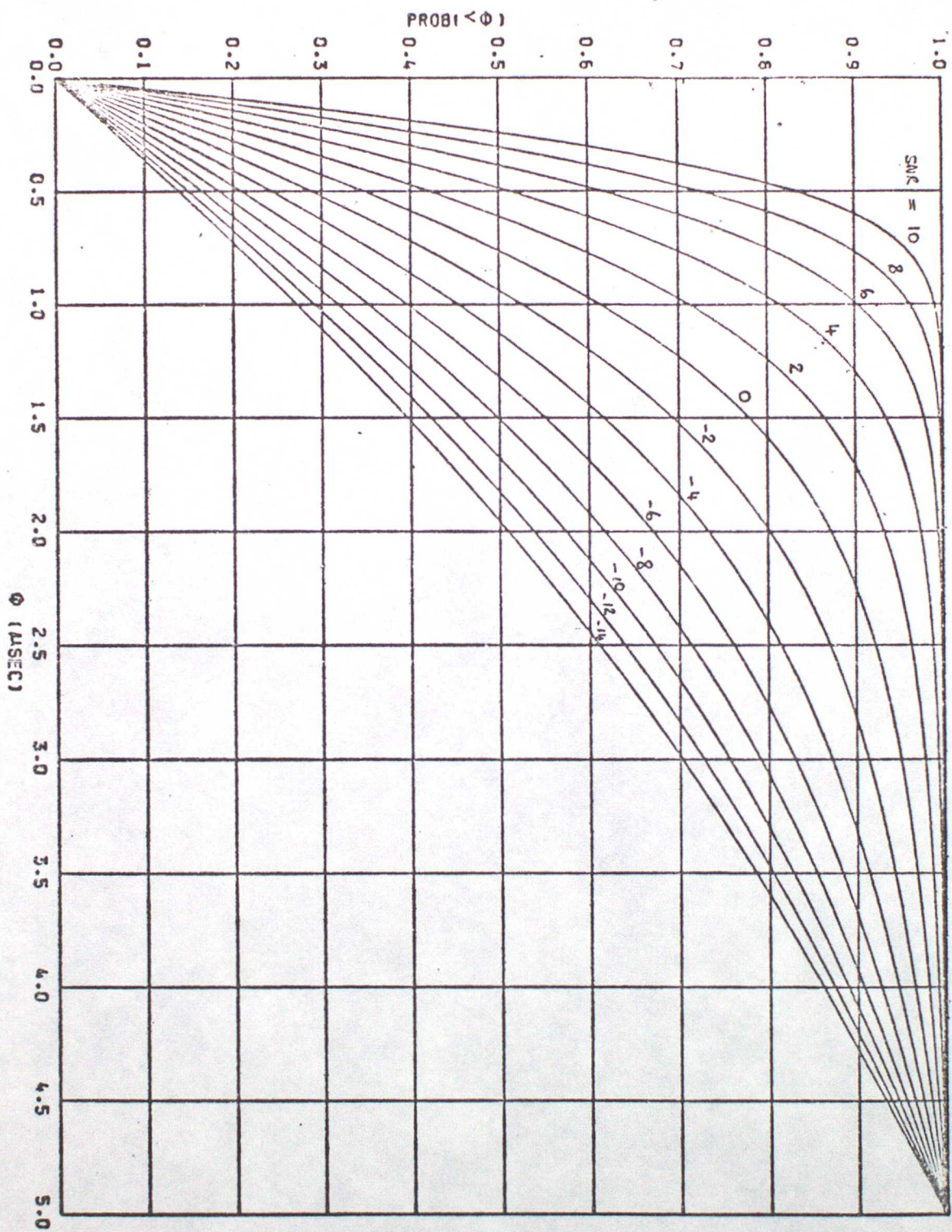


FIGURE 1 VARIATION OF PROBABILITY WITH PHASE ERROR AS A FUNCTION OF SNR

FIGURE 2 PROBABILITY THAT ERROR WILL BE LESS THAN OR EQUAL TO Φ AS A FUNCTION OF SNR



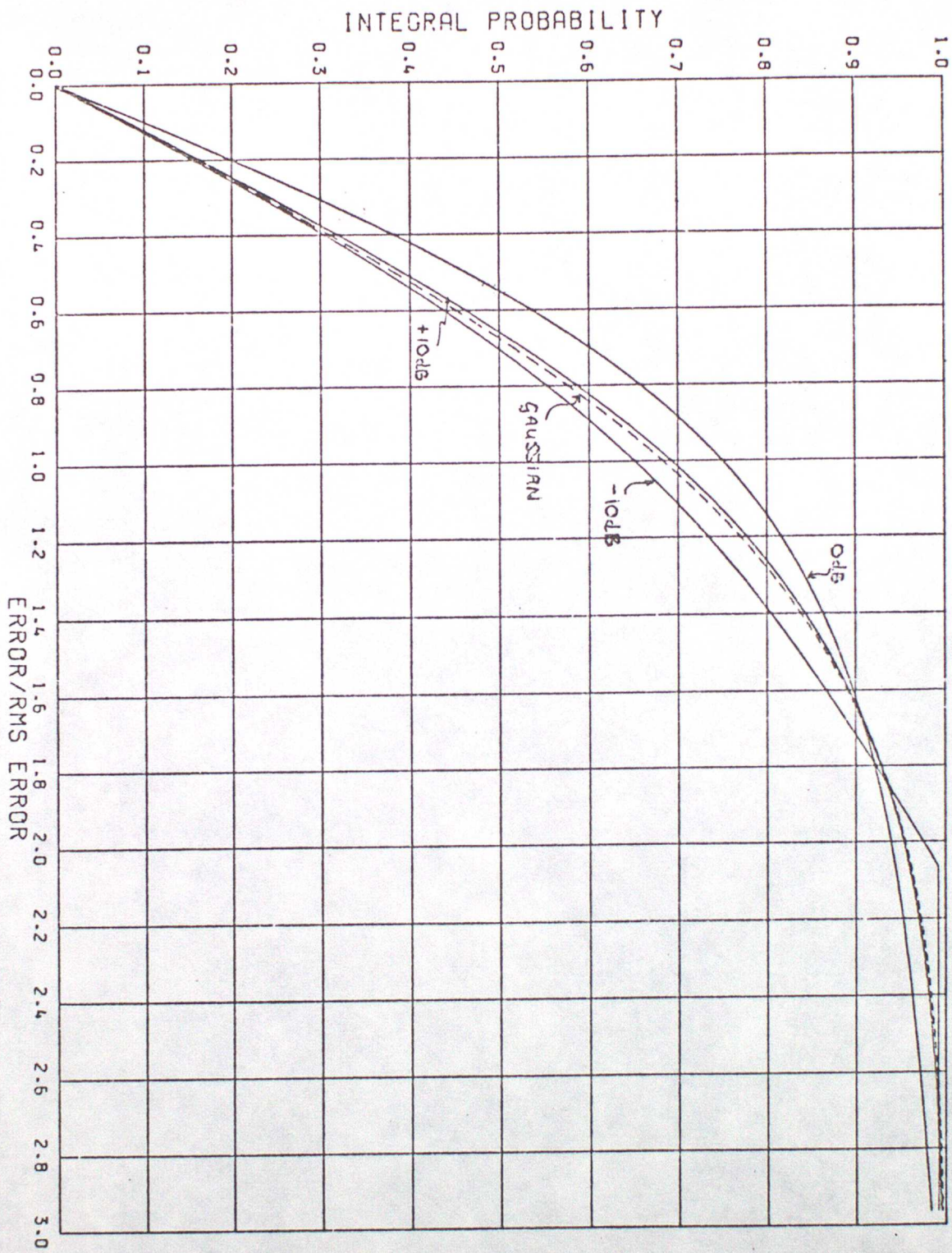


FIGURE 3 COMPARISON OF NORMALISED GAUSSIAN DISTRIBUTION AND PHASE ERROR DISTRIBUTION

1 SECOND POSITION ERROR

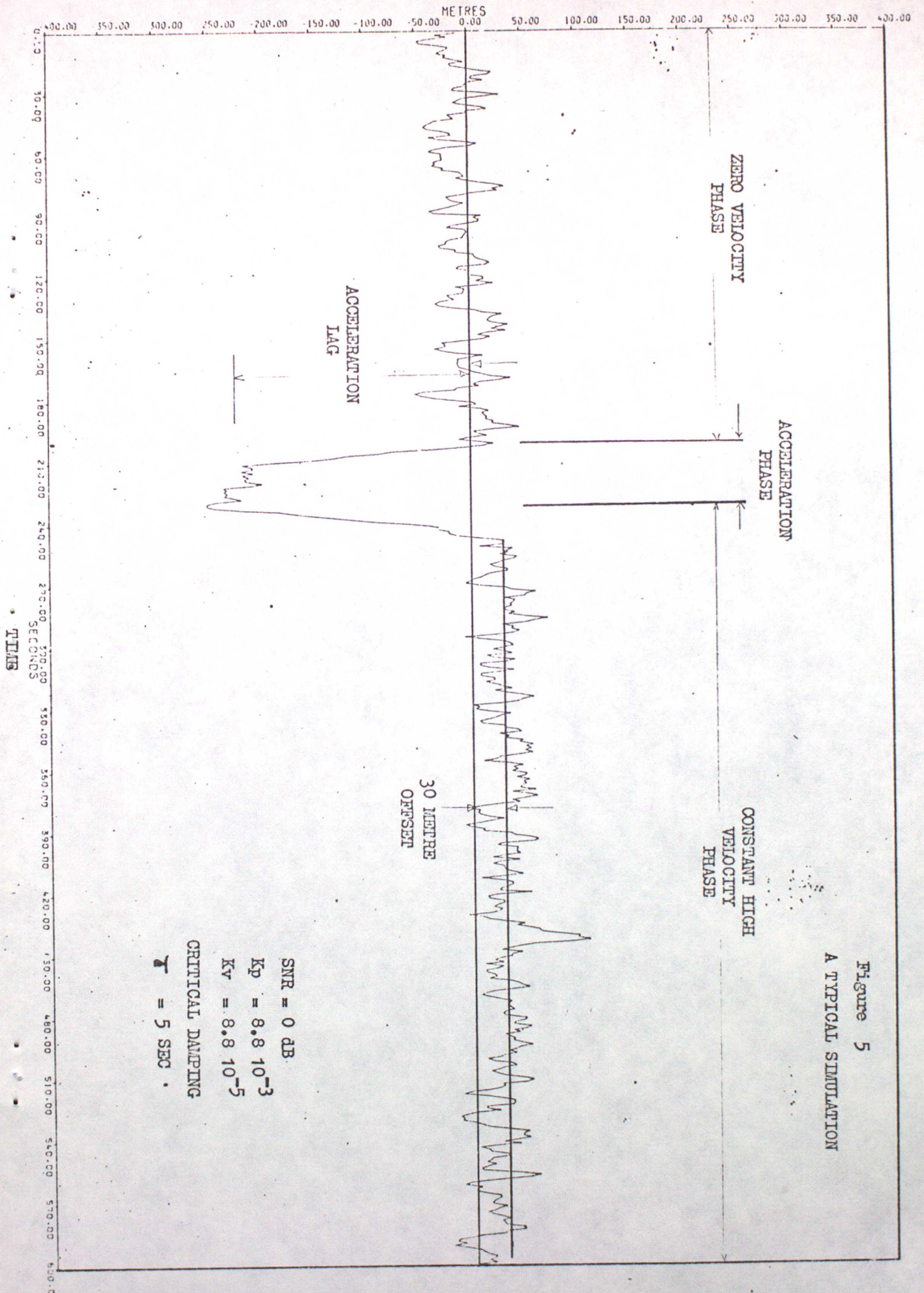
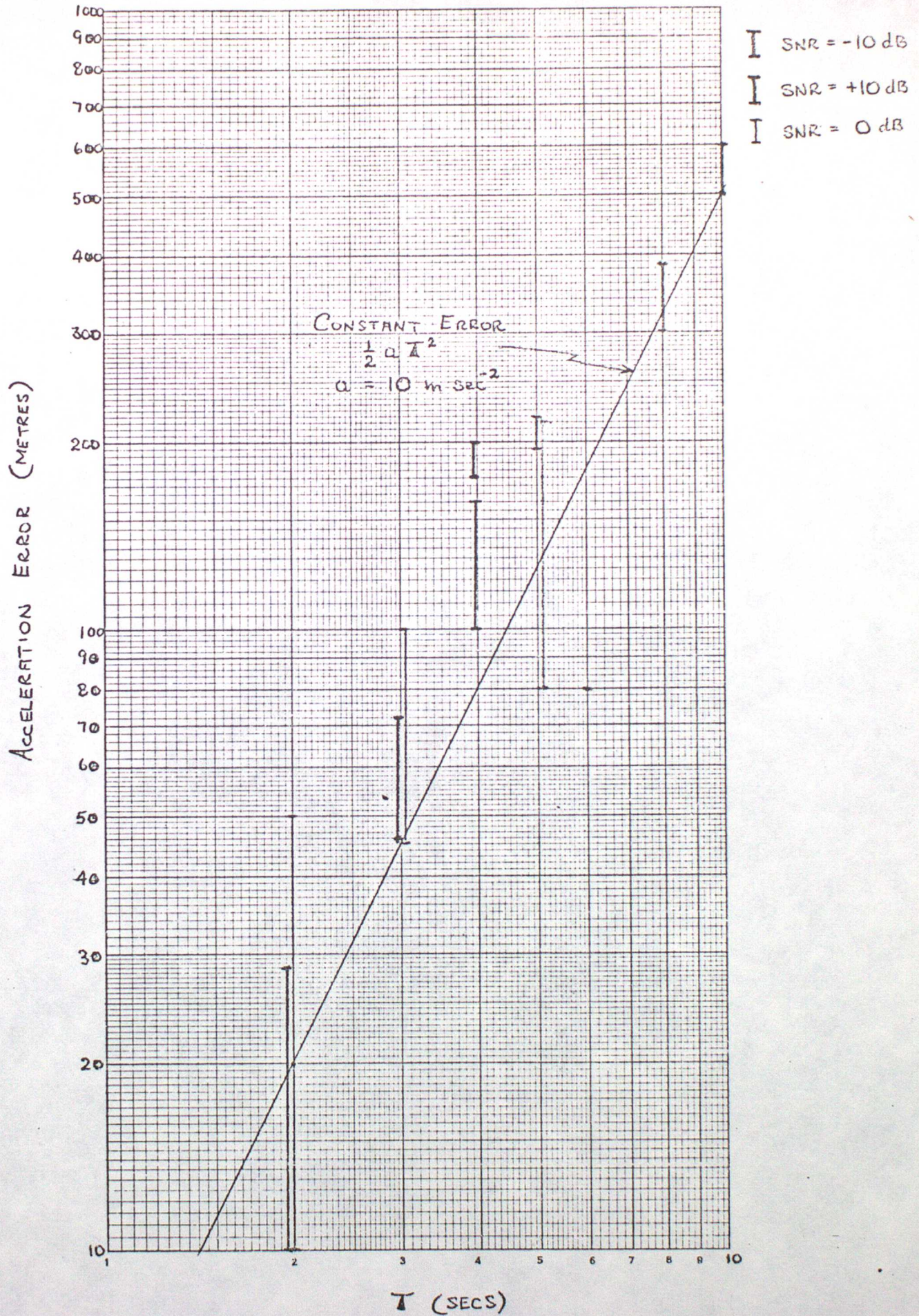


Figure 5
A TYPICAL SIMULATION

Figure 6. COMPARISON OF THE THEORETICAL, AND SIMULATED
 ERROR DURING CONSTANT ACCELERATION FOR CRITICAL
 DAMPING

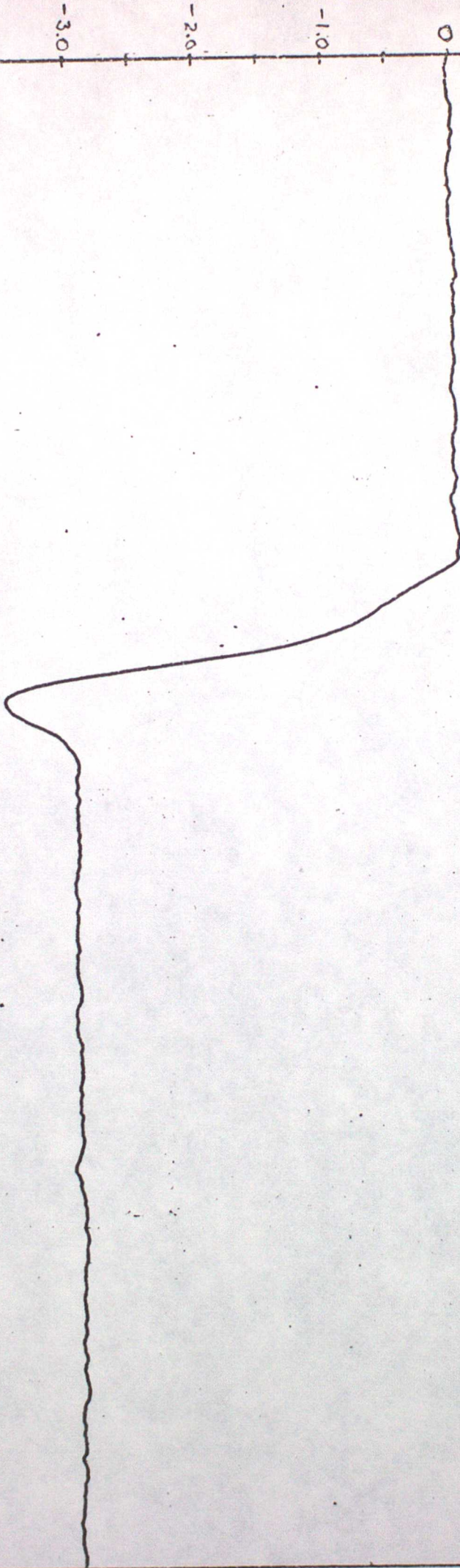


POSITION ERROR (Km)

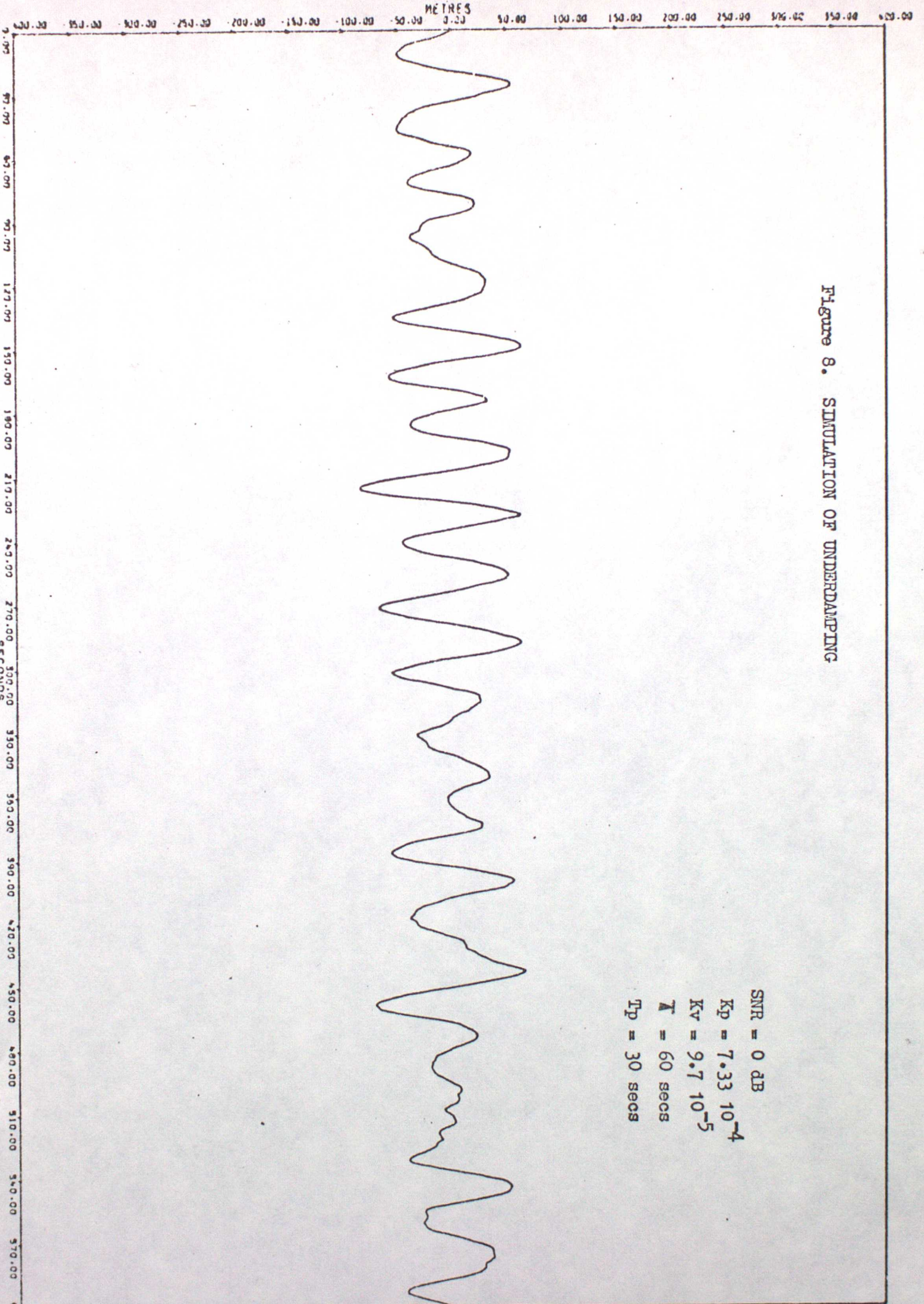
Figure 7. THE PHENOMENA OF LOSS OF LOCK DURING ACCELERATION

SNR = 0.0 dB
 $K_p = 4.4 \cdot 10^{-3}$
 $K_v = 4.0 \cdot 10^{-5}$

TIME (MINUTES)

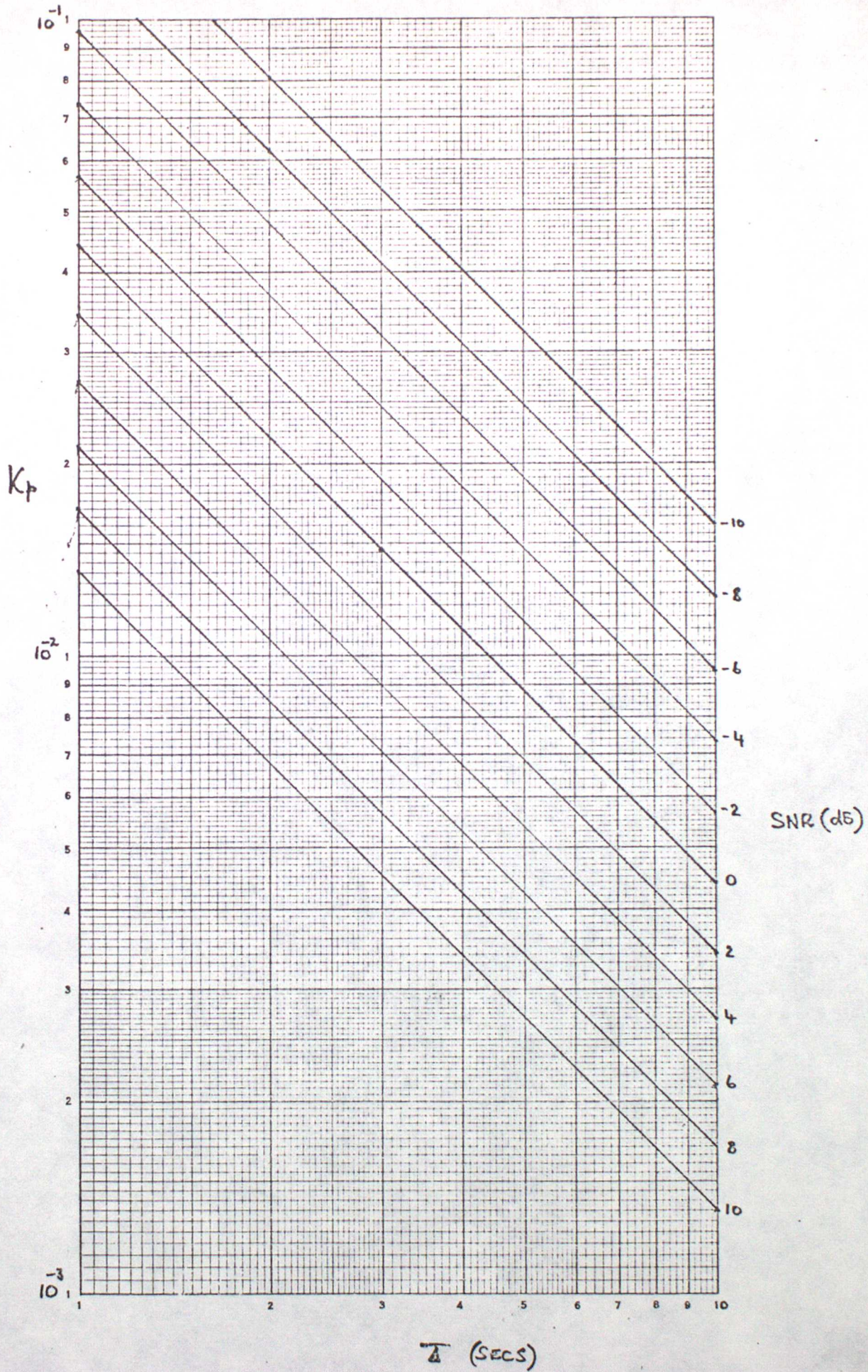


1 SECOND POSITION ERROR



ITM

Figure 9. VARIATION OF K_p WITH T FOR A RANGE OF SNRs

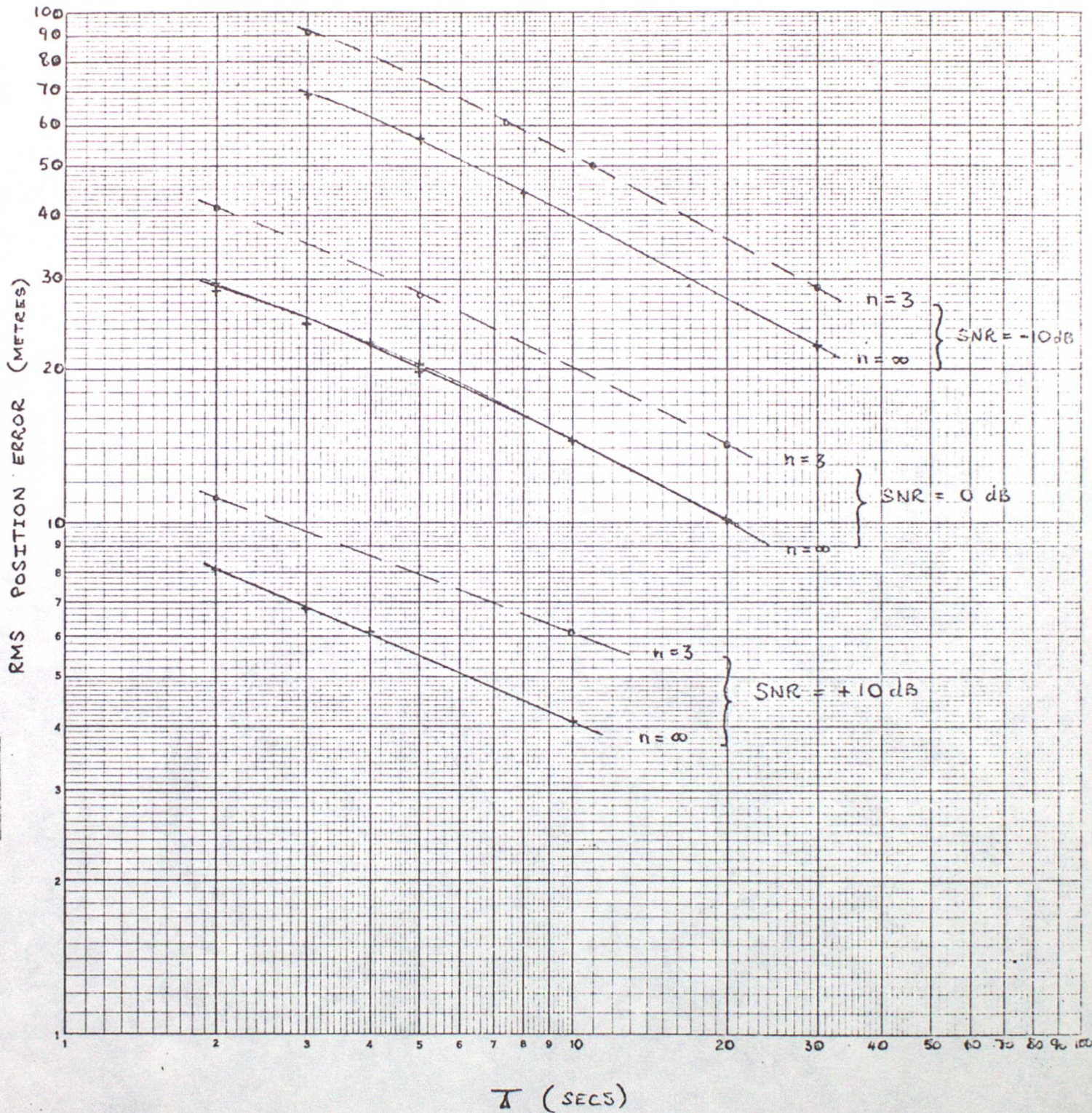


Log 2 Cycles x 1 Cycle

Graph Data Ref. 5921



Figure 10. VARIATION OF ZERO VELOCITY RMS 1 SEC POSITION ERROR AS A FUNCTION OF τ FOR A RANGE OF SNRs.



Log 2 Cycles x 2 Cycles

Graph Data Ref. 5922

WELL 10518

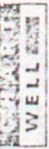
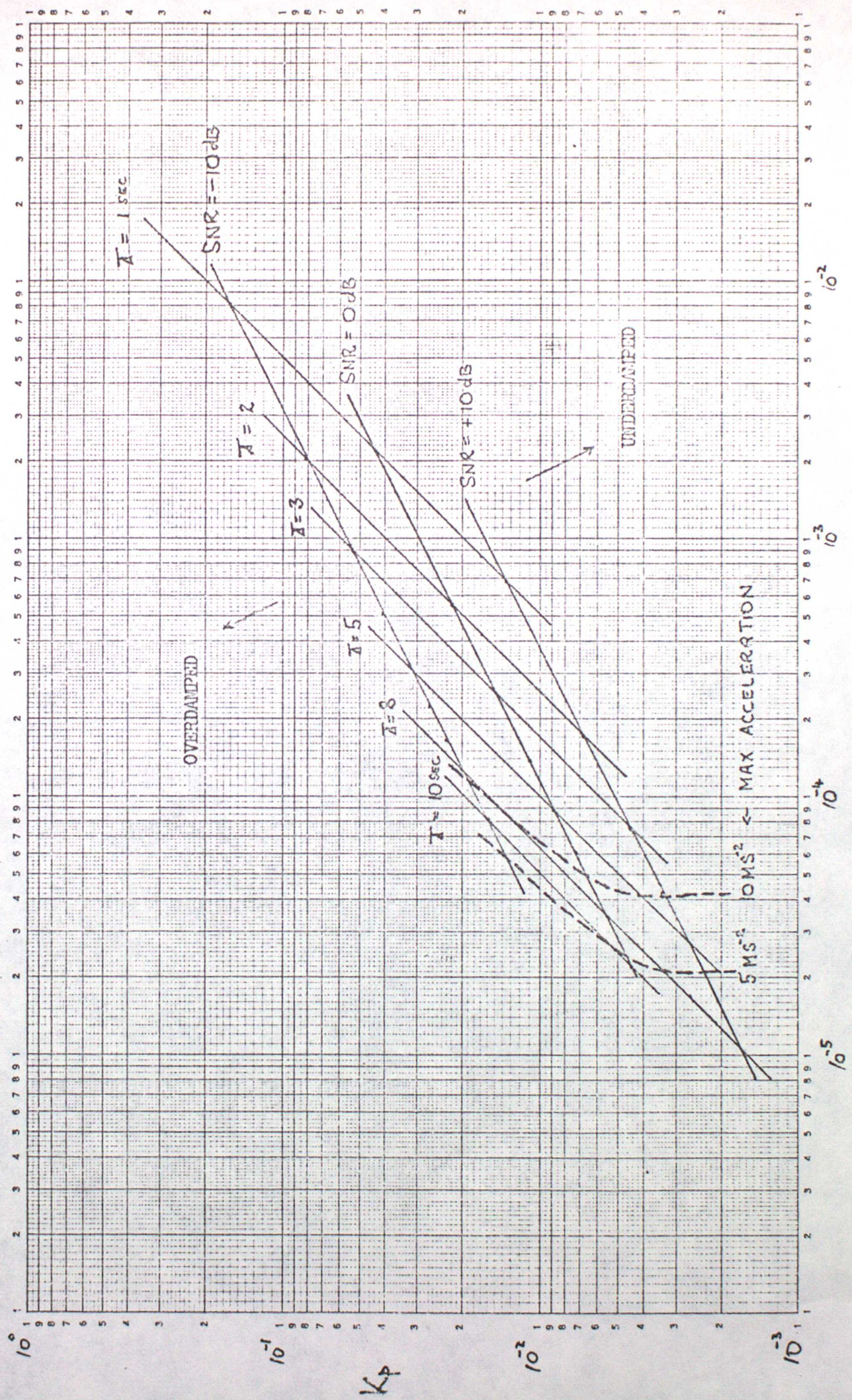


Figure 11. VARIATION OF K_p AND K_v TO PRODUCE CRITICAL DAMPING



1 SECOND POSITION ERROR

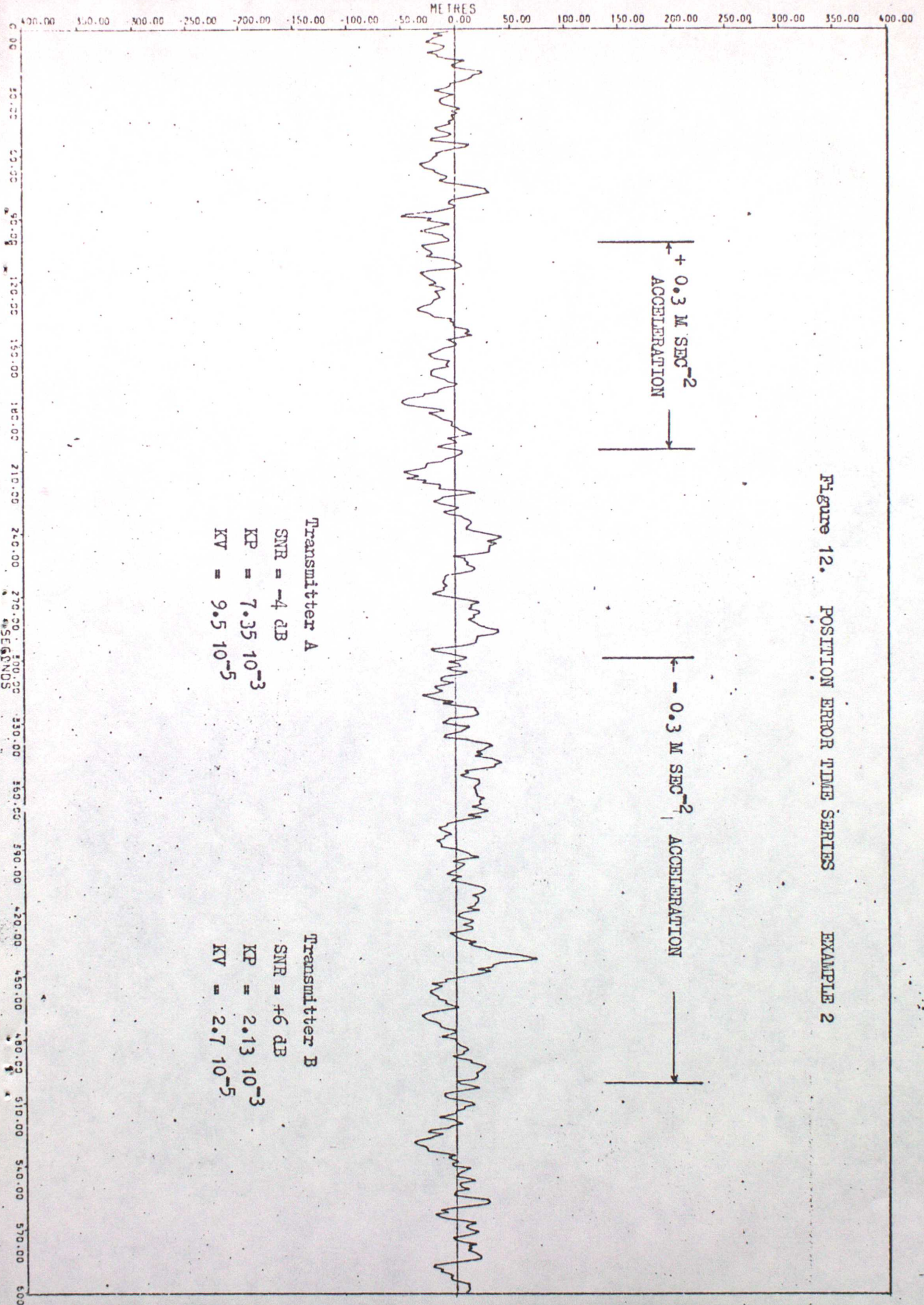


Figure 12. POSITION ERROR TIME SERIES EXAMPLE 2

Transmitter A

SNR = -4 dB
 KP = $7.35 \cdot 10^{-3}$
 KV = $9.5 \cdot 10^{-5}$

Transmitter B

SNR = +6 dB
 KP = $2.13 \cdot 10^{-3}$
 KV = $2.7 \cdot 10^{-5}$

1 SECOND POSITION ERROR

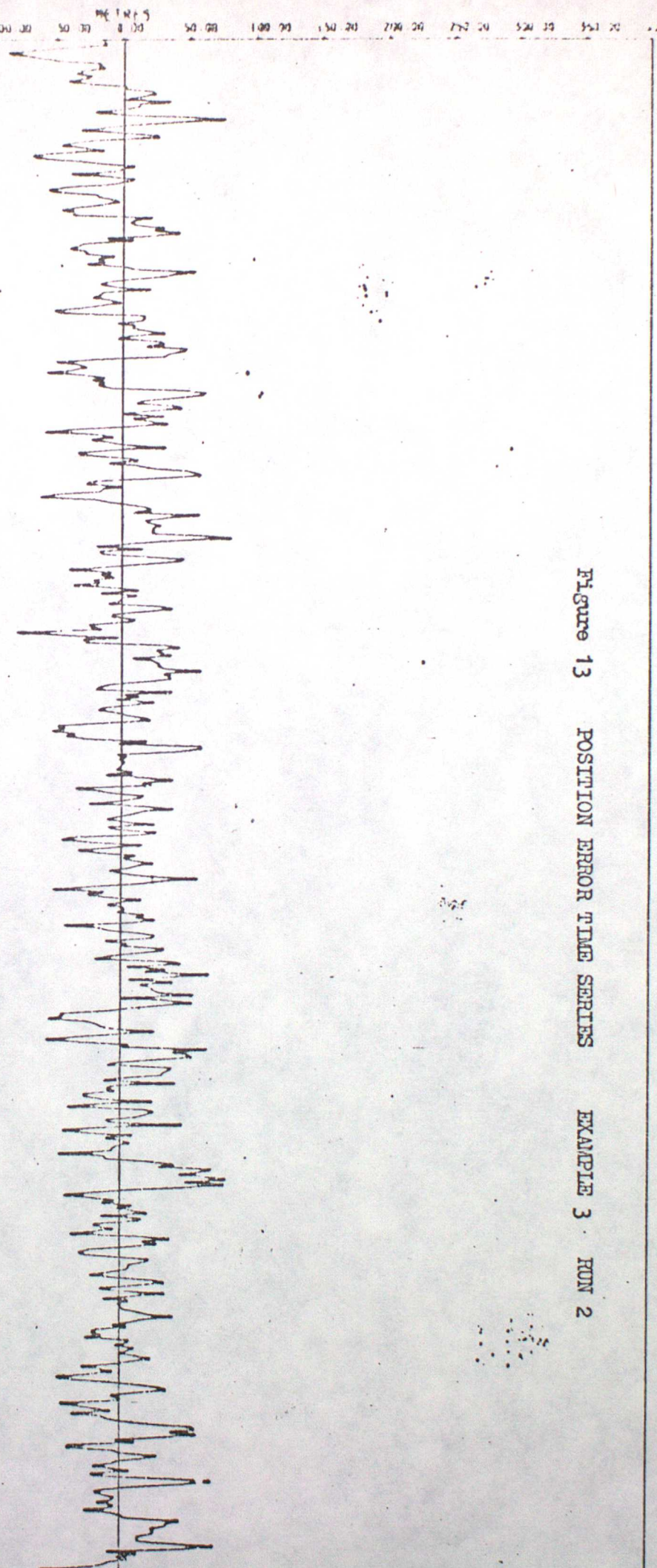


Figure 13 POSITION ERROR TIME SERIES EXAMPLE 3 RUN 2

TOA STARTING POINT = + 3.0 μ sec
 VEIL STARTING POINT = 0.0 μ sec/sec

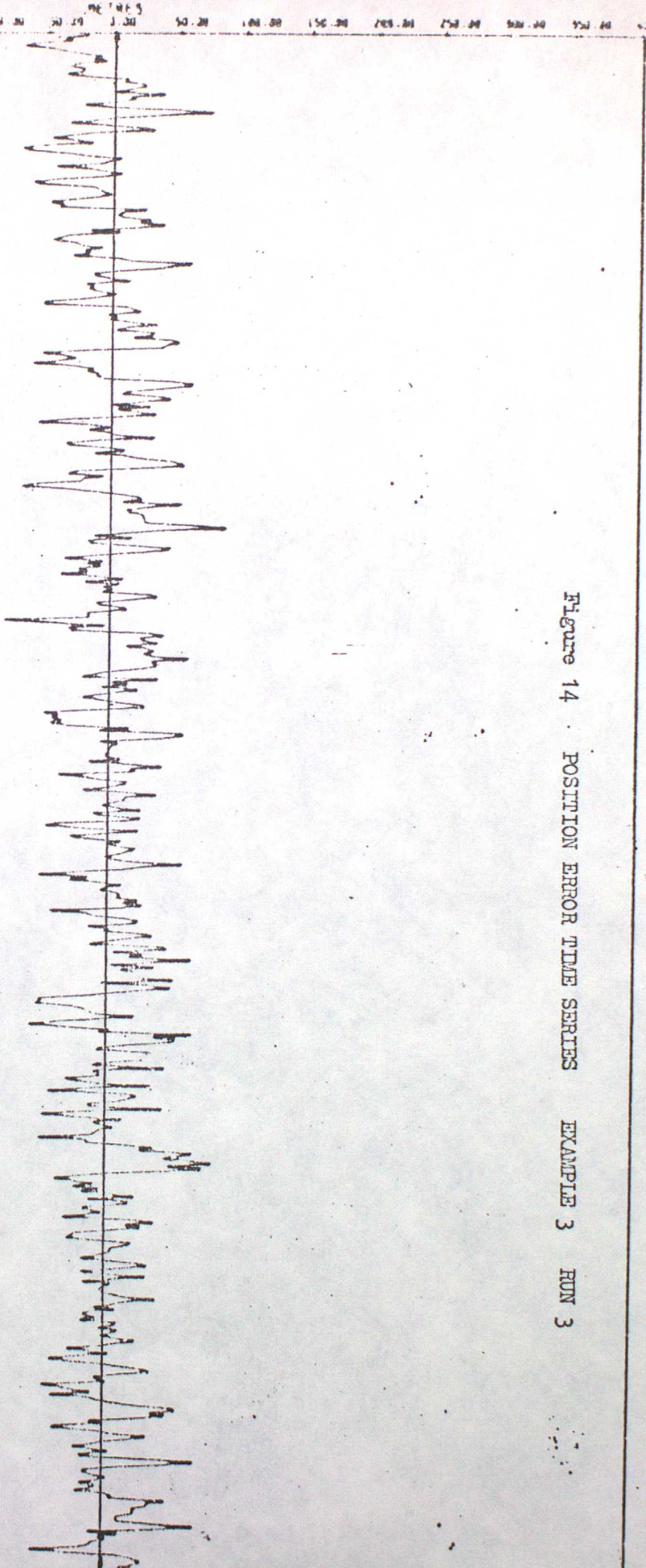
Transmission 1	Transmission 2
SNR = +6 dB	SNR = -4 dB
$K_D = 7.1 \cdot 10^{-3}$	$K_D = 2.45 \cdot 10^{-2}$
$K_V = 1.18 \cdot 10^{-4}$	$K_V = 4.08 \cdot 10^{-4}$

TIME (SECS)

0.00 0.30 0.60 0.90 1.20 1.50 1.80 2.10 2.40 2.70 3.00 3.30 3.60 3.90 4.20 4.50 4.80 5.10 5.40 5.70

1 SECOND POSITION ERROR

Figure 14 POSITION ERROR TIME SERIES EXAMPLE 3 RUN 3



TOA STARTING POINT = + 3.0 μ sec
 VEL STARTING POINT = + 0.5 μ sec/sec

Transmission 1	Transmission 2
SNR = +6 dB	SNR = -4 dB
$K_p = 7.1 \cdot 10^{-3}$	$K_p = 2.45 \cdot 10^{-2}$
$K_v = 1.18 \cdot 10^{-4}$	$K_v = 4.08 \cdot 10^{-4}$

TIME 0.00 0.10 0.20 0.30 0.40 0.50 0.60 0.70 0.80 0.90 1.00 1.10 1.20 1.30 1.40 1.50 1.60 1.70 1.80 1.90 2.00 2.10 2.20 2.30 2.40 2.50 2.60 2.70 2.80 2.90 3.00 3.10 3.20 3.30 3.40 3.50 3.60 3.70 3.80 3.90 4.00 4.10 4.20 4.30 4.40 4.50 4.60 4.70 4.80 4.90 5.00

1 SECOND POSITION ERROR

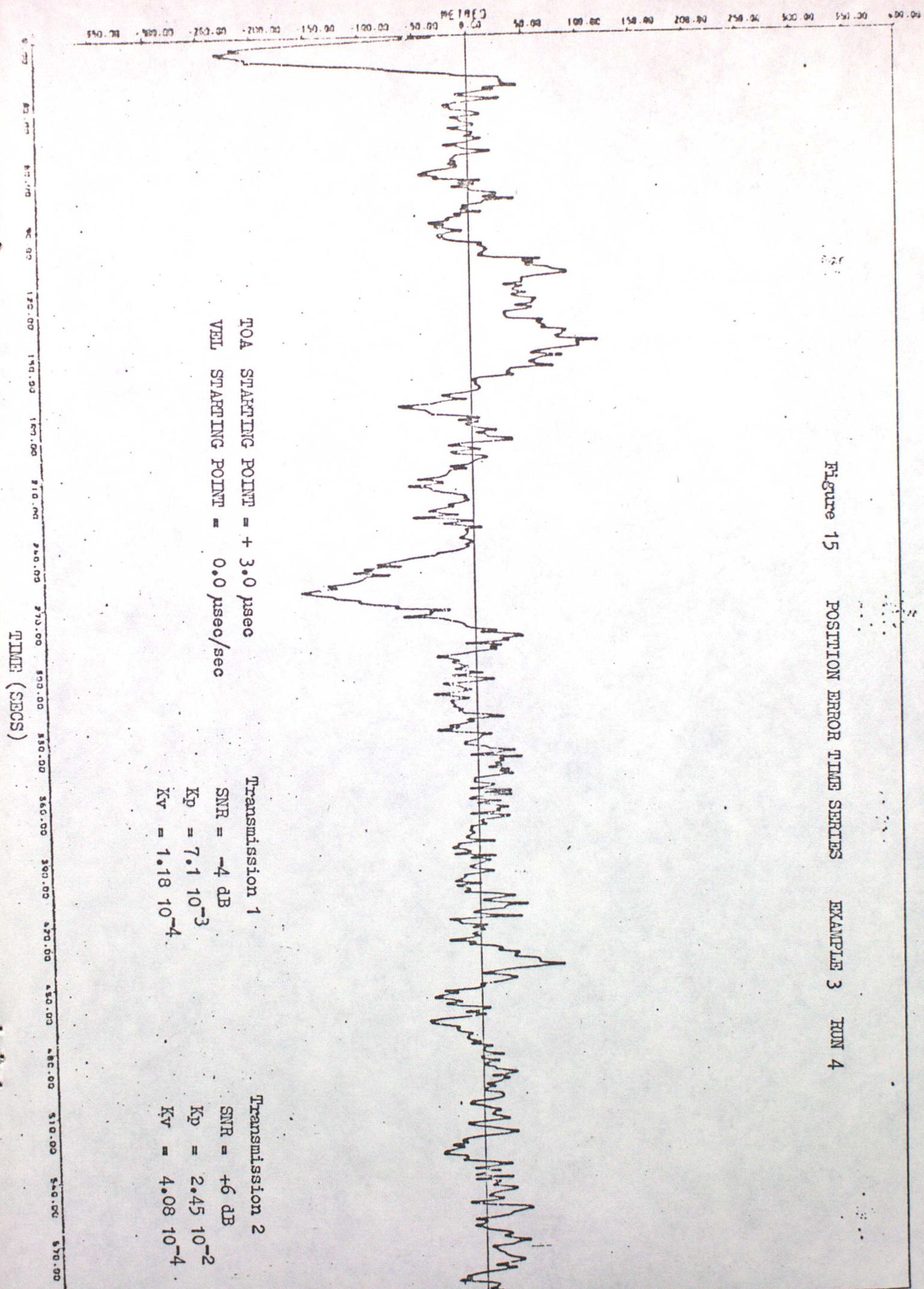


Figure 15 POSITION ERROR TIME SERIES EXAMPLE 3 RUN 4

TOA STARTING POINT = + 3.0 µsec
 VEL STARTING POINT = 0.0 µsec/sec

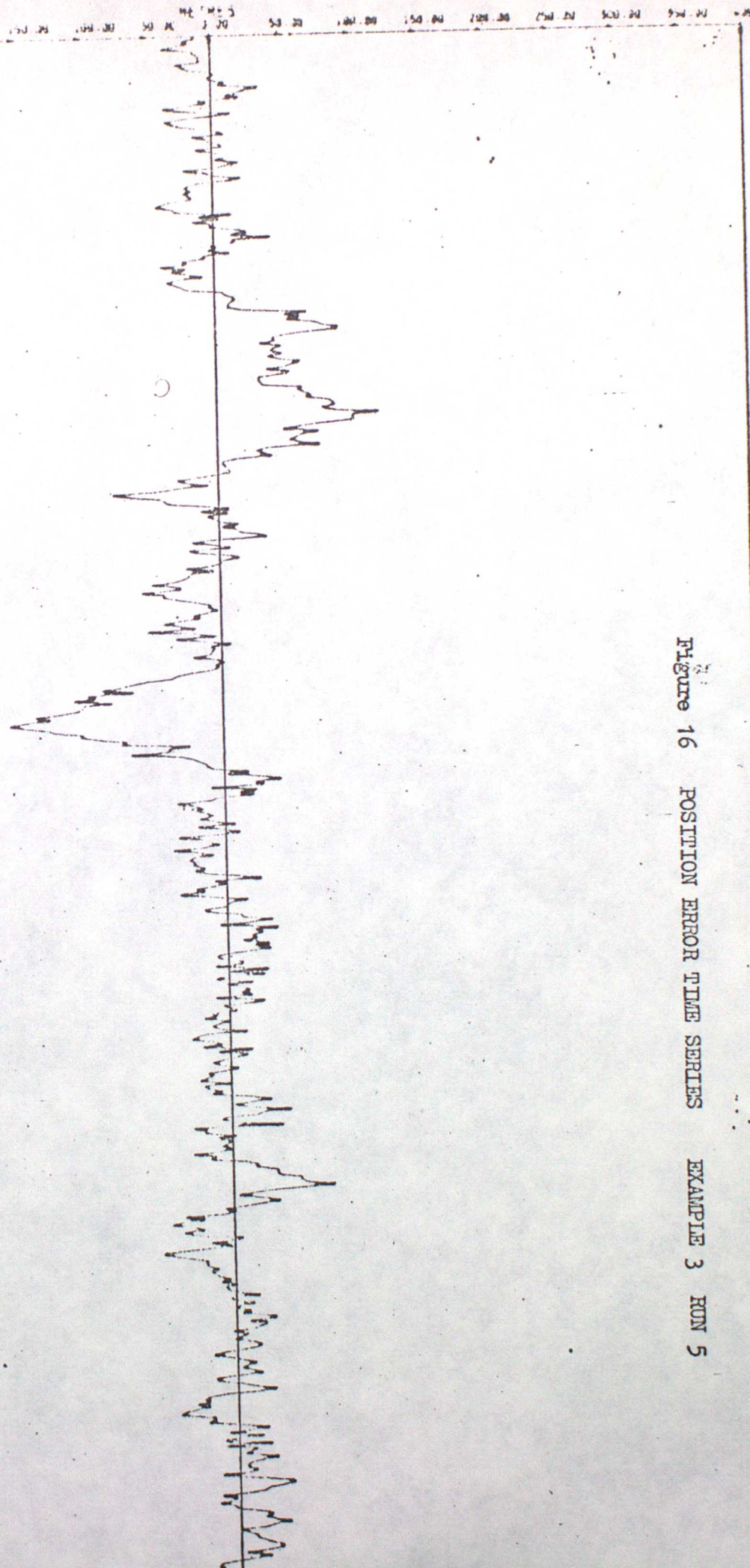
Transmission 1
 SNR = -4 dB
 $K_p = 7.1 \cdot 10^{-3}$
 $K_v = 1.18 \cdot 10^{-4}$

Transmission 2
 SNR = +6 dB
 $K_p = 2.45 \cdot 10^{-2}$
 $K_v = 4.08 \cdot 10^{-4}$

TIME (SECS)

1 SECOND POSITION ERROR

Figure 16 POSITION ERROR TIME SERIES EXAMPLE 3 RUN 5



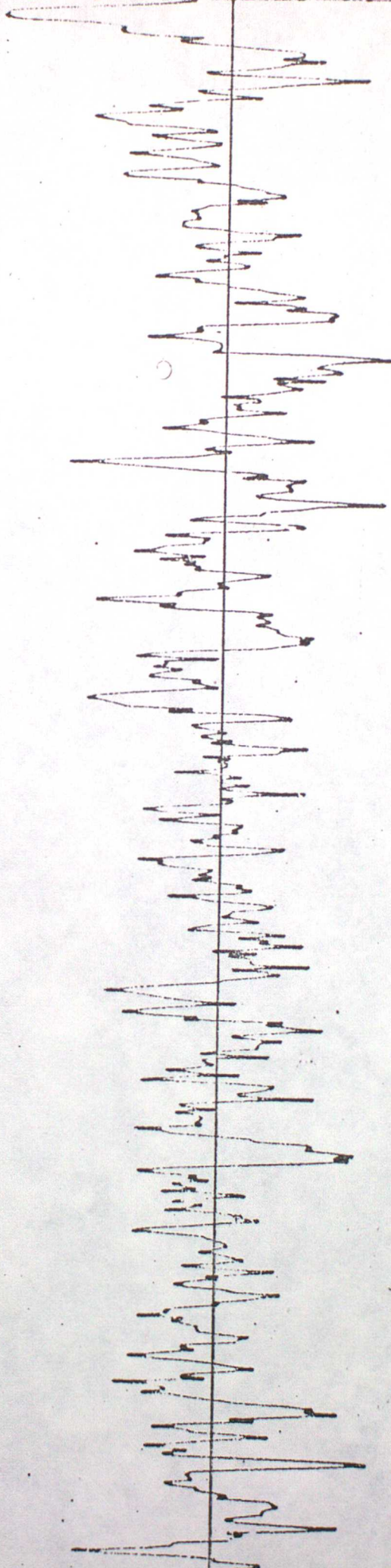
TOA STARTING POINT = + 3.0 μ sec
VEL STARTING POINT = + 0.5 μ sec/sec

Transmission 1
SNR = -4dB
 $K_p = 7.1 \cdot 10^{-3}$
 $K_v = 1.18 \cdot 10^{-4}$

Transmission 2
SNR = +6dB
 $K_p = 2.45 \cdot 10^{-2}$
 $K_v = 4.08 \cdot 10^{-4}$

1 SECOND POSITION ERROR

Figure 17 POSITION ERROR TIME SERIES EXAMPLE 3 RUN 6



TOA STARTING POINT = + 3.0 μ sec
VEL STARTING POINT = + 0.0 μ sec/sec

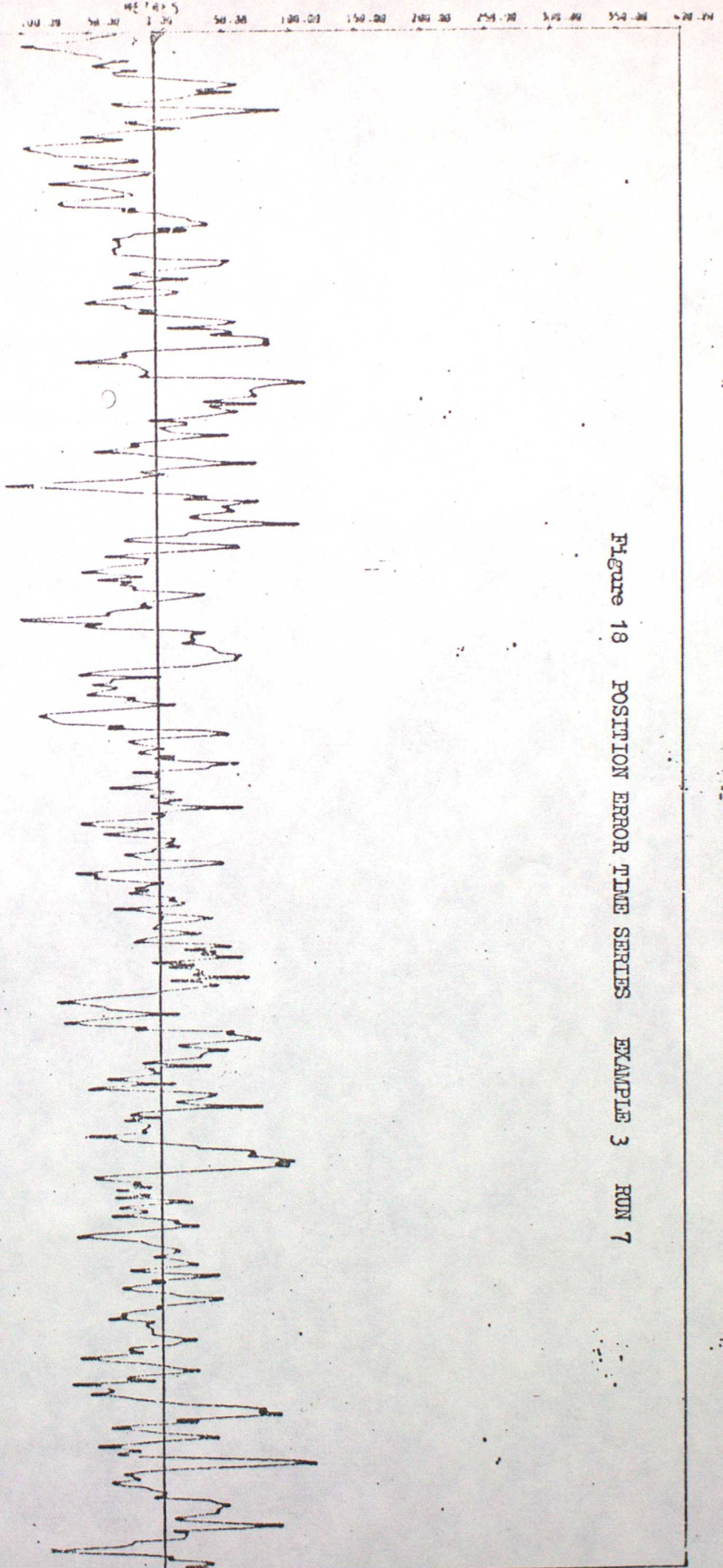
Transmission 1
SNR = 0dB
 $K_p = 7.1 \cdot 10^{-3}$
 $K_v = 1.18 \cdot 10^{-4}$

Transmission 2
SNR = -10dB
 $K_p = 2.45 \cdot 10^{-2}$
 $K_v = 4.08 \cdot 10^{-4}$

0.00 100.00 200.00 300.00 400.00 500.00
SEC

1 SECOND POSITION ERROR

Figure 18 POSITION ERROR TIME SERIES EXAMPLE 3 RUN 7



TOA STARTING POINT = + 3.0 psec
 VEL STARTING POINT = + 0.5 psec/sec

Transmission 1
 SNR = 0dB
 $K_p = 7.1 \cdot 10^{-3}$
 $K_v = 1.18 \cdot 10^{-4}$

Transmission 2
 SNR = -10dB
 $K_p = 2.45 \cdot 10^{-2}$
 $K_v = 4.08 \cdot 10^{-4}$

00:00 00:10 00:20 00:30 00:40 00:50 01:00 01:10 01:20 01:30 01:40 01:50 02:00 02:10 02:20 02:30 02:40 02:50 03:00 03:10 03:20 03:30 03:40 03:50 04:00 04:10 04:20 04:30 04:40 04:50 05:00